Received April 13, 2020, accepted April 30, 2020, date of publication May 6, 2020, date of current version May 20, 2020.

Digital Object Identifier 10.1109/ACCESS.2020.2992899

Robust Pitching Disturbance Force Attenuation for Tractor Considering Functional Constraints

GURUDATTA M. ANCHE, K. B. DEVIKA, AND SHANKAR C. SUBRAMANIAN
Department of Engineering Design, IIT Madras, Chennai 600036, India
Corresponding author: Shankar C. Subramanian (shankarram@iitm.ac.in)

ABSTRACT Tractors are attached with function-specific implements with the help of an electro-hydraulic hitch system, to carry out various farm operations. Forces arising during travel with the lifted implement on uneven terrain, generate disturbance forces on the hitch system. In this study, the electro-hydraulic system was controlled such that the disturbance forces are attenuated. A second order transfer function model of the hitch system was obtained using experimental data. In order to account for the nonlinearities in the system, an advanced Sliding Mode Controller with Power Rate Exponential Reaching Law was developed to control the hitch system to attenuate the disturbance forces. Variation in system parameters due to change of implements was taken into account by making the system adaptive using a Recursive Least Squares (RLS) parameter estimator, which was used to estimate and update the system parameters in the controller. Position regulation was incorporated to prevent the implement from reaching its mechanical limits. Valve deadzone and operating input limits were incorporated into this design. Also, considering the presence of two valves to supply fluid to the same cylinder, a trigger logic was developed to suitably choose the valve to be operated. The controller was found to provide an average disturbance force attenuation of 82.9% while being robust to a random variation in each parameter up to $\pm 80\%$.

INDEX TERMS Deadzone compensation, farm tractor, parameter estimation, pitch plane stability, sliding mode control.

I. INTRODUCTION

Farm tractors are one of the most important components in the agricultural industry and an essential part of farm mechanization. Their versatility makes them suitable for a wide variety of farm operations with different implements attached to them. In a country like India, where 54.6% of the population is engaged in agriculture [1], tractors have a significant impact on agricultural production. Even though India has the largest area of cultivated land [1] followed by the United States [2] and China [3], it is in the eight position in the world in terms of total tractor usage [4]. This difference in the number of tractors means that there is a huge scope for growth. As a consequence of this, the tractor industry is growing at an average rate of 9% per year [5], and this growth is expected to continue till 2030 [4]. With the growing numbers, it becomes important that greater focus is given to the ergonomic and technological aspects of the tractor. Sim *et al.* [6] pointed out that even with all the technological advancement, the level of comfort in tractors is less compared to other automobiles. Several studies have been conducted to understand the effect of tractor driving on the human body. Results have shown that exposure to vibration has harmful effects on the operator. Over 80% of tractor drivers reported back pain and low back pain [7]. Low-frequency vibrations during the tractor ride were found to cause discomfort to the driver with a possibility of spinal injury [8]. In tractors and off-road machinery, the low-frequency oscillations in the range of 1 Hz to 10 Hz were mainly caused due to road undulations [9].

Most tractors carry implements depending on the operations to be performed at the farm. Figure 1 shows a tractor with an implement attached at the rear through a three-point linkage, which is in turn connected to an electronically controlled hydraulic system. This hitch system can be controlled to lift and lower the implement as per the requirement. When the tractor travels on-road or between farms, the implement is lifted and held in a fixed position with respect to the tractor body. During on-road travel, it is subjected to oscillations in the pitch plane as illustrated in Fig. 1, caused due to the road undulations and the overhanging implement. These low-frequency oscillations may become severe enough to lift

The associate editor coordinating the review of this manuscript and approving it for publication was Moussa Boukhnifer.

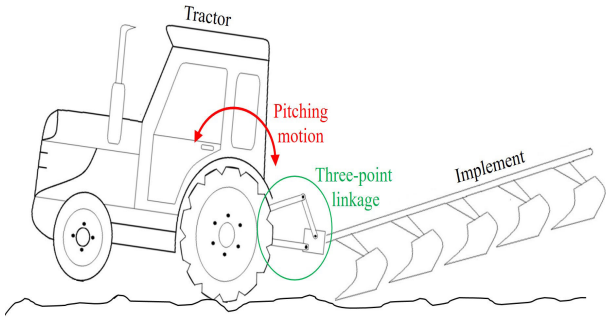

FIGURE 1. Pitch plane oscillations in a tractor with implement.

the front wheel off the ground. This causes loss of vehicle stability and steer-ability while causing discomfort to the operator. To counter the oscillations, weights are added to the front of the tractor in some instances that, however, increases fuel consumption.

The pitch plane oscillations occur not only in tractors but also in other off-road hydraulic machinery like excavators, wheel loaders, and cranes. The issue of pitch plane oscillation can be resolved by passive damping and active damping. In passive damping, either the hydraulic cylinder was maintained at a higher pressure or hydraulic accumulators were used [10], [11]. The issues with passive damping are that they are slow to respond and are suitable for a narrow range of operating conditions. In active damping, instead of keeping the implement in a fixed position, it was moved up or down according to the measured disturbances in a manner that the reaction forces transmitted to the tractor body are reduced, thereby reducing the pitching motion. Ramfled and Ivantysynova [12] studied the issues in various off-road machinery and summarized the state of the art techniques used for oscillation damping. Several active damping techniques were developed in which systems were equipped with sensors to measure quantities like pressure in the cylinder, force on the hitch, acceleration of the links, displacement or velocity of the hydraulic piston, and the position of the links. Any of these measurable quantities can be controlled such that the pitch plane oscillations are minimized. PID controllers were developed to control the force on the top link [13], [14] and acceleration of linkages [15]–[18]. Andersen *et al.* [19] used a proportional controller with a 180° phase shift to counteract the measured pitch angle acceleration. A static output feedback system that included the actuator dynamics was developed by Williamson *et al.* [20] to control the pressure in the cylinder and a similar fuzzy proportional integral (PI) controller was developed by Yang [21] and Li [22]. A model-independent PD controller with extremum seeking algorithm and gain scheduling for controlling pressure in hydraulic cranes was developed by Christofori *et al.* [10]. It was clearly seen that PID was the widely used control technique. Another important observation was that the controller parameters in most cases were fixed. Since the tractor operates in varying conditions, a set of fixed controller parameters may not perform effectively. In some recent studies, though a few gain scheduling and fuzzy based approaches were included, no attempt has been made to develop an online adaptive system. Although oscillation damping is possible by controlling various quantities in the hydraulic system, realizing them requires the use of additional sensors and hardware. Position regulation has to be incorporated in the design because it can prevent the implement from reaching its mechanical limits while working alongside oscillation damping. Additionally, a majority of the tractors have two hydraulic valves to pump and drain the hydraulic fluid respectively. During oscillation damping, it is necessary for both the valves to operate. A trigger logic has to be developed to decide the appropriate usage of the valves. This aspect, however, has not been explicitly considered in the available literature.

Based on these insights obtained from the literature, the current study aims to develop a robust control system that makes use of the existing sensors and hardware to attenuate the road disturbances. The model used for control design has been calibrated using experimental data. The proposed solution includes a Power Rate Exponential Reaching Law (PRERL) SMC, which is an advanced nonlinear control strategy applied for the first time in tractor pitch control. RLS parameter estimators have been used to make the control system adaptive to variations in system parameters that are caused due to change of implements. Position regulation was developed to prevent the implement from reaching its mechanical limits and causing structural damage to the tractor. Deadzone compensation was incorporated to compensate for the valve deadzone and improve the effectiveness of the controller. Also, considering the presence of two valves, a trigger logic was developed to suitably choose the valve to be operated and to make the best use of the system to attenuate the disturbances. Table 1 gives a comparison of the existing techniques specific to hitch control and the current study in terms of their technical attributes. Few applications of latest techniques in hydraulic control can be found in [24]–[27].

A. OBJECTIVES AND SCOPE

The objective of the study is to develop a robust control system to attenuate the disturbance forces. The system should operate within its design constraints and consider actuator attributes.

The scope of the study includes:

- Modelling the electro-hydraulic hitch system based on experimental data obtained from existing sensors on the tractor.
- Development of a controller for disturbance attenuation.
- Development of a trigger logic to switch between lifting and lowering systems during disturbance attenuation.
- Development of a parameter estimator to estimate the model parameters online and update the control input.
- Development of a position monitoring system to ensure that the implement stays within its mechanical bounds.
- Consideration of actuator properties like deadzone and operating input range.

TABLE 1. Literature comparison.

Author	Quantity controlled	Control technique	Attributes			
			Position regulation	Trigger logic	Adaptation type	Deadzone compensation
Maichle [23]	Force	P	No	No	None	No
Mizui [15]	Acceleration	NA	No	No	None	No
Berger and Patel [16]	Acceleration	P	No	No	None	No
Orbach and Schubert [13]	Force and Position	P	**Yes**	No	None	No
Patel et al. [14]	Force and Position	PD	**Yes**	No	None	No
Andersen et al. [19]	Pressure and Pitch angle	P	**Yes**	No	None	No
Yang [21]	Pressure and Position	Fuzzy PID	No	No	None	No
Williamson et al. [20]	Pressure	Static Output Feedback	No	No	None	No
Christofori et al. [10]	Pressure	PD	No	No	**Offline**	No
Zhang and Chen [17]	Vertical acceleration	PID	No	No	None	No
Alexander et al. [18]	Acceleration and Pressure	PD	No	No	**Offline**	No
Current study	Force and Position	SMC	**Yes**	**Yes**	**Online**	**Yes**

NA - Not Available, SMC - Sliding Mode Control

Though the study is primarily associated with farm tractors equipped with an electro-hydraulic hitch system to carry implements, the concept can also be applied to other off-road hydraulic machinery that are used to carry loads.

B. PROPOSED SOLUTION

A block diagram of the proposed system is shown in Fig. 2. It comprises three major parts, namely, position control, force control, and parameter estimation. Based on the external disturbance $\Delta f_d(t)$ and the change in force feedback ($\Delta f(t)$), the trigger logic decides between lifting and lowering to attenuate the disturbance. Once lifting or lowering has been selected, the corresponding states are estimated, using which the control input ($u_{li}(t)$ or $u_{lo}(t)$) is evaluated. The controller and estimator are designed separately for lifting and lowering. The subscripts *li* and *lo* refer to lifting and lowering respectively. The parameter estimator uses the control input and change in force output to estimate the model parameters and update them in the controller. The position control circuit uses the measured position $\phi(t)$ to check if the implement stays within the allowable range. Based on the information obtained from the position monitoring system, if position control needs to be carried out, then the corresponding current input is provided to the valves. Details about the design and development of the model and control system are discussed in the following sections.

II. SYSTEM MODELLING

A schematic diagram of a typical electro-hydraulic hitch system used in tractors is shown in Fig. 3. It consists of a hydraulic pump to supply the hydraulic fluid to the cylinder through the valves. The rod end of the cylinder is connected to a three-point linkage on which the implement is mounted. Two valves are used for lifting and lowering the implement. The lifting control valve supplies the fluid to the cylinder and the lowering control valve drains the fluid from the cylinder. Currents $u_{li}(t)$ and $u_{lo}(t)$ indicate the input given to the lifting and lowering valves respectively. Lifting or lowering of the implement changes its position with respect to the tractor and the force acting on the hitch point. The system is equipped with a force sensor to measure the force acting on the top link $f(t)$, and a position sensor to measure the angle of the top link $\phi(t)$. It was observed that a nominal force acts on the top link when the implement is mounted. This force changes only when the lifting or lowering action takes place and remains nearly constant during the rest of the time. In order to capture this change in force as a response to the input current,

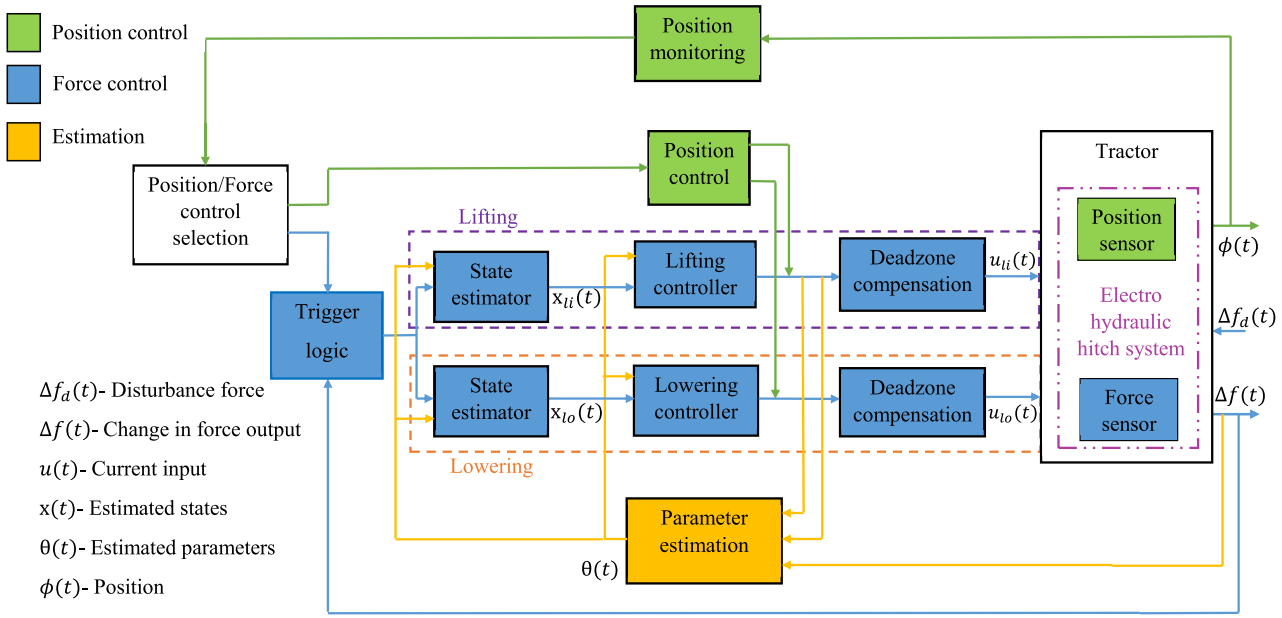

FIGURE 2. System block diagram.

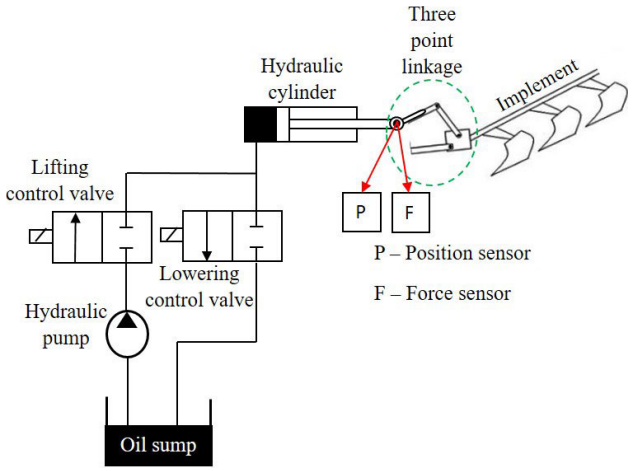

FIGURE 3. Electro-hydraulic hitch system.

the nominal force was subtracted from the instantaneous force to obtain the change in force $\Delta f(t)$. By analyzing the frequency response, the system was approximated to be a Linear Time Invariant (LTI) system [28]. Further, the system model used in this study was represented through a transfer function, with current as input and change in force $\Delta f(t)$ as output.

The electro hydraulic system was modelled using data obtained from an experimental setup. The system was reasonably approximated to be linear time invariant by analysing its frequency response. The response of the system to a step current input was used to obtain the transfer function parameters. Initially the system was modelled using a first-order transfer function model [28]. The same experimental data was further used to improve the accuracy of the model by considering a second-order transfer function. Accuracy was quantified using mean absolute percentage error (MAPE) given by

$$\text{MAPE} = \left[\frac{1}{N}\sum_{i=1}^{N}\frac{f_{exp}(i) - f_{sim}(i)}{f_{exp}(i)}\right]100, \tag{1}$$

where N is the number of samples, f_{exp} is the experimental response and f_{sim} is the simulated response. The model accuracy was found to improve by 31% with the use of a second order model. The systematic procedure followed to obtain second-order model parameters was reported [29], and the model obtained is given by,

$$\frac{\Delta F(s)}{I(s)} = \frac{K{\omega_n}^2 s}{s^2 + 2\zeta\omega_n^2 s + {\omega_n}^2}, \tag{2}$$

where $\Delta F(s)$ is the change in force output (N), $I(s)$ is the current input (A), ζ is the damping ratio, ω_n is the natural frequency (rad/s) and K is the system gain (N/A). The results obtained are shown in Table 2. A comparison between experimental response and theoretical response for 2.5 A input is shown in Figs. 4 and 5. It has to be noted that the input was given to the lifting valve and the lowering valve as two separate entities and they had different characteristics. This made them behave as two different systems. Therefore, it was required to model the system and develop the estimator and the controller for lifting and lowering individually.

III. CONTROLLER DESIGN

The primary objective of the control system is to regulate the hitch system such that the measured disturbance force is driven to 0 N. Additionally, the control system has to

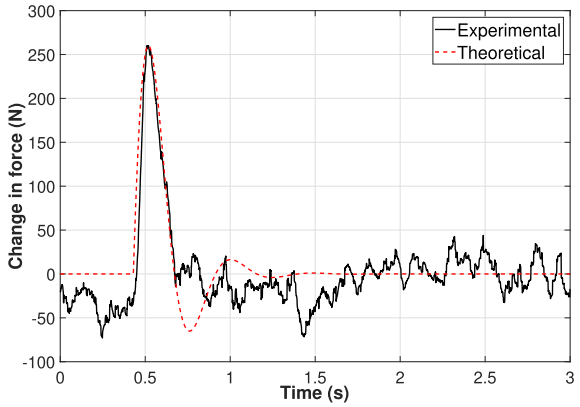

FIGURE 4. Comparison of experimental and theoretical response (lifting) [29].

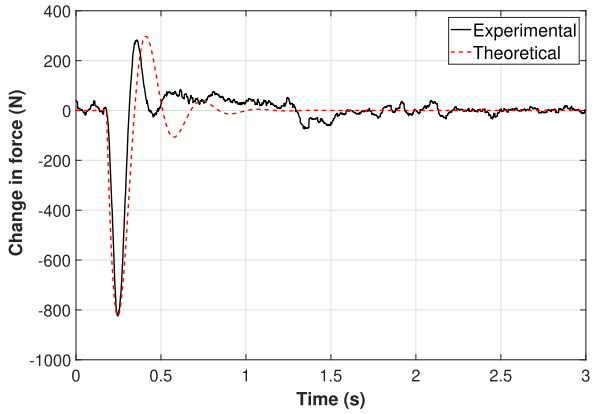

FIGURE 5. Comparison of experimental and theoretical response (lowering) [29].

TABLE 2. Model parameters [29].

Parameter	Lifting	Lowering
ω_n (rad/s)	14.18	20.19
ζ	0.403	0.309
K (N/A)	19.10	-41.28

incorporate the aspects stated in the objectives. The procedure followed is discussed in the following sections.

A. STATE ESTIMATION

A state estimator is required to estimate the states of the system that would be useful in calculating the control input. The state space representation of the transfer function in Eq. 2 can be written as

$$\dot{\mathbf{x}}(t) = \mathbf{A}\mathbf{x}(t) + \mathbf{b}u(t), \tag{3}$$

$$y(t) = \mathbf{c}.\mathbf{x}(t), \tag{4}$$

where $\mathbf{x}(t) \in \mathbb{R}^n$, $\mathbf{A} = \begin{bmatrix} 1 & 0 \\ -\omega_n^2 & -2\zeta\omega_n \end{bmatrix}$, $\mathbf{b} = \begin{bmatrix} 0 \\ 1 \end{bmatrix}$ and $\mathbf{c} = \begin{bmatrix} 0 \\ K\omega_n^2 \end{bmatrix}$. The Kalman filter was used for state estimation [30], [31]. Two state estimators were developed and tuned for lifting and lowering. In a comparison between estimated output and experimental data, an average estimation error evaluated using MAPE was found to be of 3.8% and 7.5% in the case of lifting and lowering respectively.

B. SLIDING MODE CONTROL

Since the tractor is operated with different implements, it is beneficial to have a controller that is robust to parameter variations. Considering its inherent robustness property and invariance towards parametric uncertainties and external disturbances [32], Sliding Mode Control (SMC) was selected. SMC finds numerous applications in real life non-linear and adaptive robust control problems [33]–[35]. The ability of SMC to ensure robustness in sliding mode and the property of order reduction in sliding mode make SMC a proficient control strategy [36]. Regardless of its advantages, chattering is a major limitation of SMC. Gao and Hung [37], [38] proposed a well known chattering mitigation strategy called the reaching law approach, of which the Constant Rate Reaching Law (CRRL) and Power Rate Reaching Law (PRRL) are conventionally used techniques. Although CRRL reduces chattering, it is to a limited extent, and PRRL is more effective at reducing chattering, but at the cost of robustness. To address this trade-off between chattering mitigation, speed of response, and robustness, Devika and Thomas [39] proposed a Power Rate Exponential Reaching Law (PRERL). It was shown to improve the speed of response and chattering alleviation while ensuring robustness. The current study is an application of this advanced SMC with PRERL in the oscillation damping domain. In the disturbance attenuation problem under consideration, the desired change in force is 0 N. Therefore, the sliding surface was chosen such that both the states $x_1(t)$ and $x_2(t)$ are driven to 0, as given by,

$$s(t) = \lambda(x_2(t) - x_{2d}(t)) + (x_1(t) - x_{1d}(t)), \tag{5}$$

where $\lambda > 0$ is the slope of the sliding surface, $x_{2d}(t) = 0$, and $x_{1d}(t) = 0$. On employing PRERL [39],

$$\dot{s}(t) = -\frac{G}{\delta_0 + (1-\delta_0)e^{-\alpha|s(t)|^p}}|s(t)|^\beta \text{sign}(s(t)), \tag{6}$$

where $G > 0$ is the controller gain, $\delta_0 < 1, \alpha, 0 < \beta < 0.5$ and p are controller parameters that have an effect on the reaching time and the extent of chattering mitigation. Evaluating $\dot{s}(t)$ from Eq. 5 and equating to Eq. 6,

$$\lambda\dot{x}_2(t) + \dot{x}_1(t) = -\frac{G}{\delta_0 + (1-\delta_0)e^{-\alpha|s(t)|^p}}|s(t)|^\beta \text{sign}(s(t)). \tag{7}$$

Simplifying Eq. 7 using Eq. 3, the control input was obtained as,

$$u(t) = \frac{1}{\lambda}\Bigg[-\frac{G}{\delta_0 + (1-\delta_0)e^{-\alpha|s(t)|^p}}|s(t)|^\beta \text{sign}(s(t)) - x_2(t) + \lambda\omega^2 x_1(t) + 2\zeta\lambda\omega x_2(t)\Bigg]. \tag{8}$$

The estimated states were used in Eq. 8 to calculate the control input. The controller parameters are given in Table 3

TABLE 3. Controller parameters.

Parameter	Lifting	Lowering
λ	1	10
G	4	5
δ_0	0.1	0.1
α	2	2
β	0.5	0.5
p	1	1

1) STABILITY ANALYSIS

Lyapunov's stability analysis [40] was carried out for the PRERL based SMC with the selected sliding surface. Using Eq. 3 and Eq. 5, $\dot{s}(t)$ can be written as,

$$\dot{s}(t) = \lambda(-\omega^2 x_1(t) - 2\zeta\omega x_2(t) + u(t)) + x_2(t) + d(t). \quad (9)$$

The variable $d(t)$ represents a bounded disturbance in the system, which could arise due to sensor noise, variations in ambient conditions, and fluctuations in system response due to extended periods of operation. A suitable Lyapunov function [41] was chosen as

$$V = \frac{1}{2}s^2. \quad (10)$$

The condition for asymptotic stability about the equilibrium point ($s^* = 0$) is given by, $\dot{V} < 0, \forall s \neq 0$. Differentiating Eq. 10,

$$\dot{V} = s\dot{s}. \quad (11)$$

Substituting Eq. 8 and Eq. 9 in Eq. 11,

$$\dot{V} = s\left(- \frac{G}{\delta_0 + (1-\delta_0)e^{-\alpha|s(t)|^p}} |s(t)|^\beta \text{sign}(s) \right) + sd(t). \quad (12)$$

Consider the magnitude of $d(t)$ to be bounded by a positive scalar D and considering $\frac{G}{\delta_0+(1-\delta_0)e^{-\alpha|s(t)|^p}}|s(t)|^\beta = \Gamma$. Equation 12 can now be written as,

$$\dot{V} < sD - s\Gamma\text{sign}(s), \quad (13)$$

which can be rewritten as,

$$\dot{V} < -|s|(\Gamma - D). \quad (14)$$

For $\dot{V} < 0, \forall s \neq 0$,

$$|s|(\Gamma - D) > 0, \quad (15)$$

$$\implies \Gamma > D. \quad (16)$$

Equation 16 gives the condition for asymptotic stability. This can be used in practice by estimating the disturbance in the system [42], [43] and choosing the controller parameters appropriately.

C. DEADZONE COMPENSATION

Deadzone is a prevalent attribute of hydraulic valves. It is the range of input values for which the system does not respond, i.e., the valves do not generate an output flow. This can be accredited to the overlap in valve spools. The overlap is typically provided to prevent leakages when the valve is closed. When the valve is actuated, the spool has to move the distance of overlap before flow occurs, which gives rise to the deadzone. This causes the system to perceive an input different from the supplied input. Also, the time taken to generate the flow induces a delay in system response [44]. In order to get a desired response from the system, it is necessary to compensate for the deadzone. The most commonly used technique is the deadzone inverse [44]–[46]. In this technique, the control input is modified such that the system receives the desired input after the effects of deadzone. The dead zone parameters can be determined experimentally [47]. However, in case of an unknown deadzone, certain adaptive control techniques that can incorporate the deadzone effects are available [48]–[50]. In hydraulic valves, deadzone typically ranges from 10% to 35% of the operating range. Valve manufacturers also specify the deadzone value for a particular valve [51]–[53]. Since the deadzone parameters were known in the current study, a simple and easily implementable fixed parameter deadzone inverse technique [45] was considered. For the system under study, the deadzone z_m was found to be 1 A [28] and the slope was taken as $m = 1$. The compensated input was calculated as,

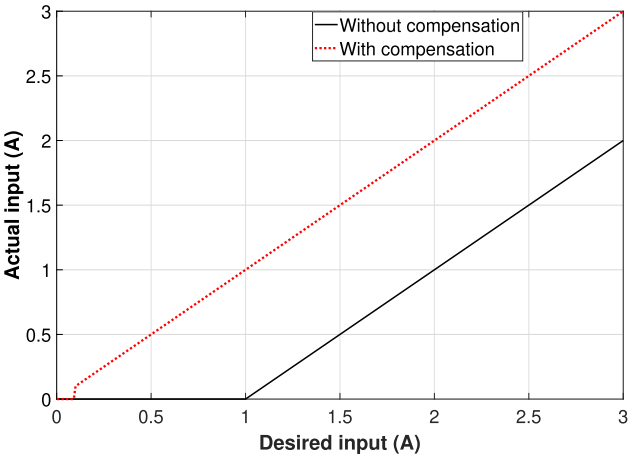

FIGURE 6. Effect of deadzone compensation.

$$u_c(t) = \begin{cases} \left(\frac{z_m + \frac{l_c}{m}}{l_c}\right)u(t), & \text{if } 0 \leq u(t) \leq l_c, \\ \frac{u(t)}{m} + z_m, & \text{if } u(t) > l_c, \end{cases} \quad (17)$$

where l_c is called the smoothness width that can be chosen by the designer depending on the capability of the hardware and extent of compensation required. In this study, $l_c = 0.1$. The effect of the dead zone compensation on the input is shown in Fig. 6. It can be seen that the deadzone effects are minimized after compensation.

D. OPERATING INPUT RANGE

The hydraulic valves have an operating current range within which the supplied input must lie. The lower bound and the upper bound for current input are denoted by u_{lb} and u_{ub}. In case of disturbance force attenuation, if the magnitude of force is high the controller may demand a current input

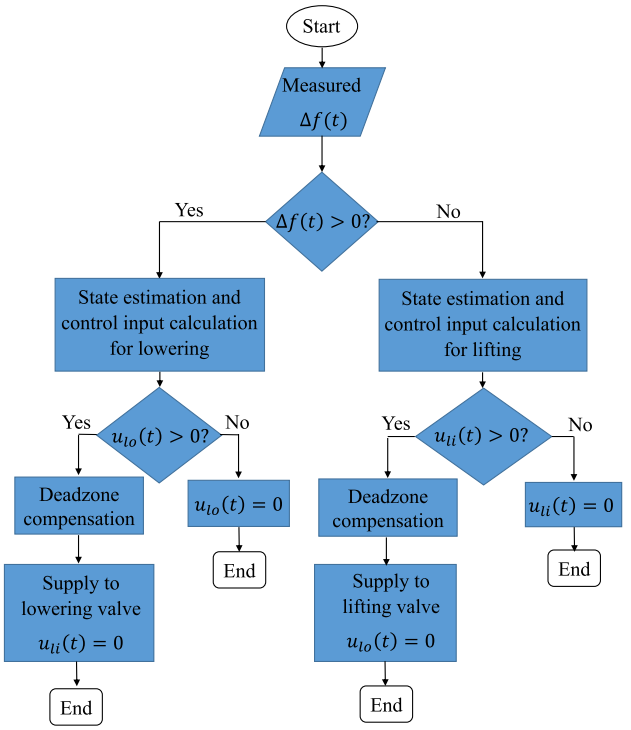

FIGURE 7. Force control flowchart.

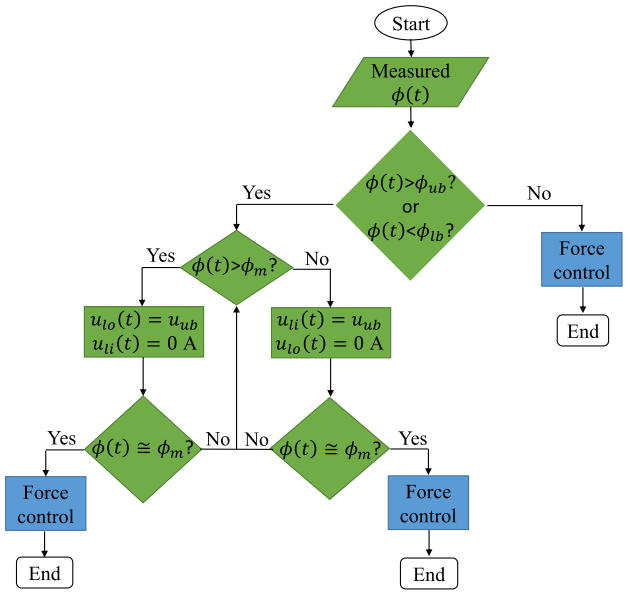

FIGURE 8. Position control flowchart.

greater than u_{ub}. One way to address this is by lowering the controller gain. It is not a feasible option to lower the controller gain as it will affect the performance at lower magnitudes of force. In order to keep the current input within operating limits, a saturation was imposed on the control input at u_{ub}. For the system under study, $u_{ub} = 3.3$ A and $u_{lb} = 0$ A.

E. TRIGGER LOGIC

As discussed earlier, lifting and lowering systems behave as separate entities. In order to accomplish effective disturbance attenuation, both systems must work in harmony. It is necessary to define a set of rules that govern the operation of either system based on the nature of the measured disturbance force. The flow chart in Fig. 7, which represents force control, shows the trigger logic that is used to decide the valve actuation. From Fig. 4 and Fig. 5, it can be observed that lifting generates a positive change in force and lowering generates a negative change in force. Based on this, in order to produce a counteracting effect, when the force was negative, the lifting system was actuated and vice versa for lowering. Once the system was selected, the states corresponding to the disturbance force were estimated and the control input was evaluated. Since the lifting and lowering valve operation was mutually exclusive, when one of the systems was active, the input to the other was set to 0 A.

F. POSITION CONTROL

The implement has an allowable range of motion between the points where it touches the ground and the mechanical stopper on the tractor. It can cause structural and functional damage to the tractor if the implement reaches its bounds on a moving tractor. It has to be ensured that the implement position is within the allowable limits. In this study, 0° to 60° was the allowable range of motion with 0° corresponding to the implement being on the ground. Keeping a margin for safety, the limits were selected to be 5°(ϕ_{lb}) and 55°(ϕ_{ub}), and 30°(ϕ_m) was considered to be the mean position for the implement. A position monitoring and control logic was developed and is shown in Fig. 8. If the measured position ($\phi(t)$) exceeds the bounds, input was supplied to the corresponding valve until the implement was brought back to the mean position. Maximum allowable current (u_{ub}) was supplied to achieve fast re-positioning of the implement. Position control has to work alongside force control. However, they cannot be active simultaneously as the control inputs from both systems should be given to the same valves. Therefore, only one of them can be active at a time. Whenever the implement exceeds the bounds, priority was given to the position controller. Force control was resumed once the implement was brought back to its mean position.

G. PARAMETER ESTIMATION

A tractor has to be attached to different implements that vary in geometry, size, and mass, depending on the operation to be carried out. This change in mass and location of center of gravity of the implement with respect to the tractor cause a change in response of the electro-hydraulic system. In the current application of oscillation damping, where the hitch has to be constantly controlled, the variation in parameters has to be accounted for in the control input provided to the actuators. Thus, it is necessary that the parameters be estimated online, so that vibration attenuation is improved, and the effort required in tuning and calibration is minimized.

TABLE 4. Parameter estimation error.

Parameter	Lifting (%)	Lowering(%)
ζ	1.36	2.82
ω	0.40	0.37
K	0.22	0.11

A recursive least squares (RLS) estimator [54], [55] was selected owing to its computational simplicity. Taking inverse Laplace transform of Eq. 2, the following equation was obtained,

$$\ddot{y}(t) + 2\zeta\omega_n\dot{y}(t) + {\omega_n}^2 y(t) = K{\omega_n}^2\dot{u}(t), \tag{18}$$

where $y(t) = \Delta f(t)$ and $u(t) = i(t)$. Writing Eq. 18 in discrete domain,

$$\begin{aligned} y_k = &\frac{2 + 2\zeta\omega_n\Delta t}{1 + 2\zeta\omega_n\Delta t + {\omega_n}^2} y_{k-1} \\ &- \frac{1}{1 + 2\zeta\omega_n\Delta t + {\omega_n}^2} y_{k-2} \\ &+ \frac{K{\omega_n}^2\Delta t}{1 + 2\zeta\omega_n\Delta t + {\omega_n}^2}(u_k - u_{k-1}), \end{aligned} \tag{19}$$

which can be rewritten as,

$$y_k = ay_{k-1} + by_{k-2} + cu_k + du_{k-1}, \tag{20}$$

with $a, b, c,$ and d being functions of parameters ζ, ω and K. Using RLS estimator with input-output data, the values of $a, b, c,$ and d were estimated, and ζ, ω, and K were calculated for lifting and lowering.The following equations were used for RLS estimator. The RLS model can be written as

$$\boldsymbol{\theta}_k = \boldsymbol{\theta}_{k-1}, \tag{21}$$

$$yk = {\boldsymbol{\psi}_k}^T\boldsymbol{\theta}_k + v_k, \tag{22}$$

where ${\boldsymbol{\psi}_k}^T = \begin{bmatrix} y_{k-1} & y_{k-2} & u_k & u_{k-1} \end{bmatrix}$ and $\boldsymbol{\theta}^T = \begin{bmatrix} a & b & c & d \end{bmatrix}$. The parameter estimates are calculated using the following. The gain ($\mathbf{k}_{p_k}$) is evaluated by,

$$\mathbf{k}_{p_k} = \frac{\mathbf{P}_{p_{k-1}}\boldsymbol{\psi}_k}{1 + {\boldsymbol{\psi}_k}^T\mathbf{P}_{p_{k-1}}\boldsymbol{\psi}_k}, \tag{23}$$

The parameter estimates are updated using the measurement by,

$$\boldsymbol{\theta}_k = \boldsymbol{\theta}_{k-1} + \mathbf{k}_{p_k}(y_k - {\boldsymbol{\psi}_k}^T\boldsymbol{\theta}_{k-1}), \tag{24}$$

The covariance matrix ($\mathbf{P}_{p_k}$) is updated using,

$$\mathbf{P}_{p_k} = (\mathbf{I} - \mathbf{k}_{p_k}{\boldsymbol{\psi}_k}^T)\mathbf{P}_{p_{k-1}}. \tag{25}$$

Figure 9 shows a comparison between the reference values from Table 2 and the estimated parameters for lifting and lowering. The average estimation error in the steady state region is shown in Table 4.

The parameter estimators for lifting and lowering must work only when the corresponding system is active. Estimating the parameters when the system is not active leads to false estimates. The estimates need to be updated in the controller only after they converge. The flow chart in Fig. 10 gives the conditions under which the parameters were estimated and updated.

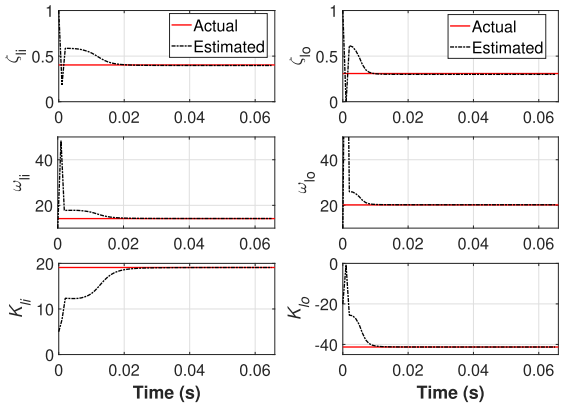

FIGURE 9. Parameter estimation comparison.

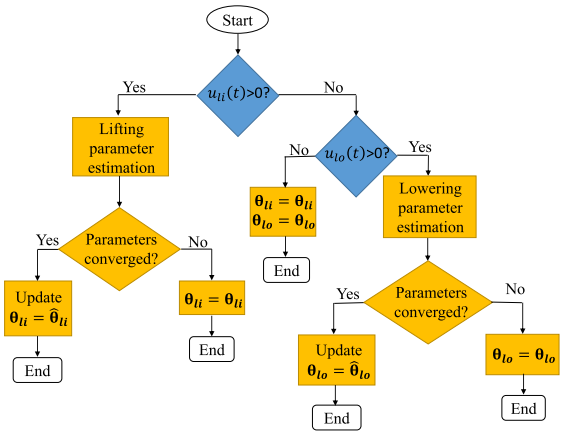

FIGURE 10. Parameter estimation flowchart.

IV. RESULTS AND DISCUSSION

The designed subsystems were integrated to form the system shown in Fig. 2. Performance analysis was carried out using a MATLAB script consisting of the equations of model, estimator and controller along with the conditions at which they are active. Velmurugan *et al.* [56] presented the experimental values of force disturbance in tractors. Zhang and Chen [17] developed a formulation to determine the vibration experienced by the tractor due to road inputs. Jaiswal *et al.* [57] developed a terrain model for a tractor with front loader. Based on these studies, the nature and magnitude of disturbances were selected. The maximum magnitude presented by Velmurugan *et al.* [56] was of the order of 1500 N. In order to test the controller for more demanding conditions, a force disturbance signal with magnitudes ranging up to 4000 N was considered in this study. The system response to the disturbance force is shown in Fig. 11. It shows a comparison between the system without control and with control using PRERL SMC. It is clearly seen that the controller attenuates the disturbance force whereas the system without control oscillates with high magnitudes of force. It can also be observed from current input that a negative force is attenuated by providing lifting current, and positive force by providing

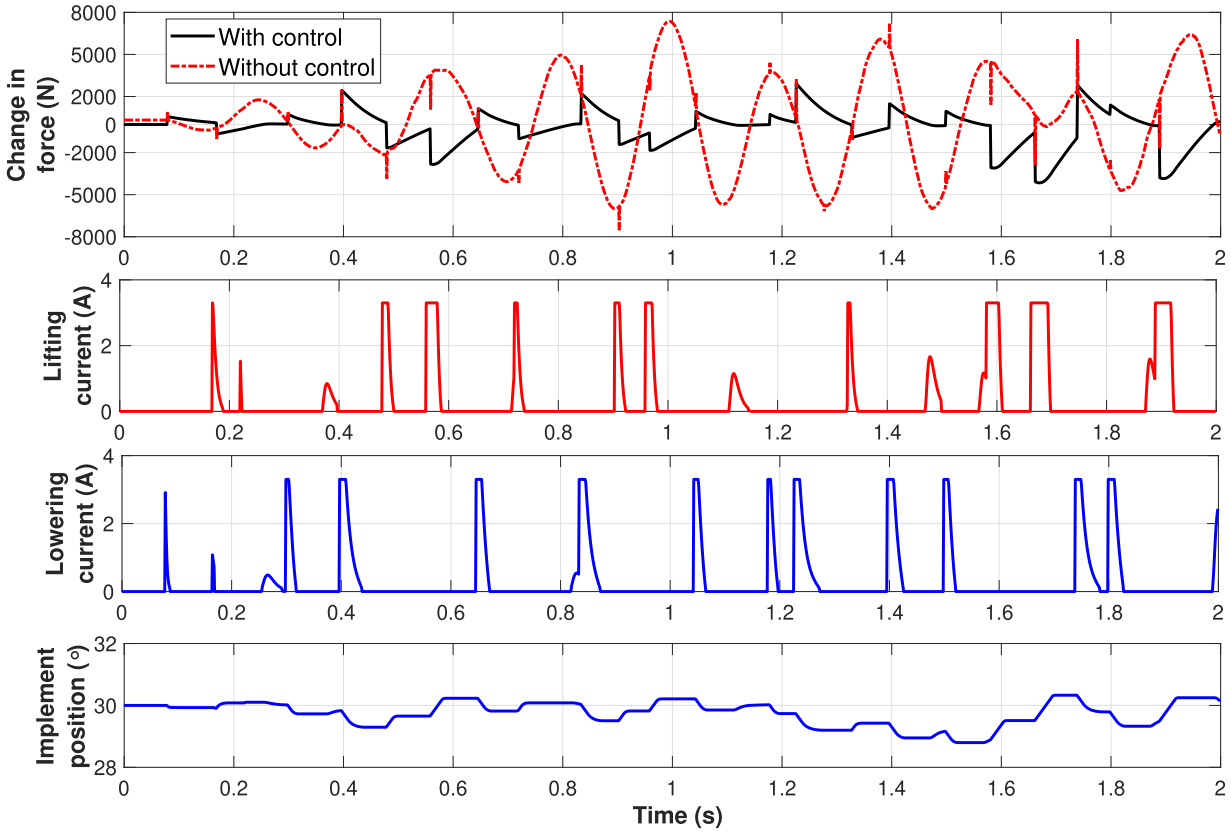

FIGURE 11. Performance comparison of the integrated system.

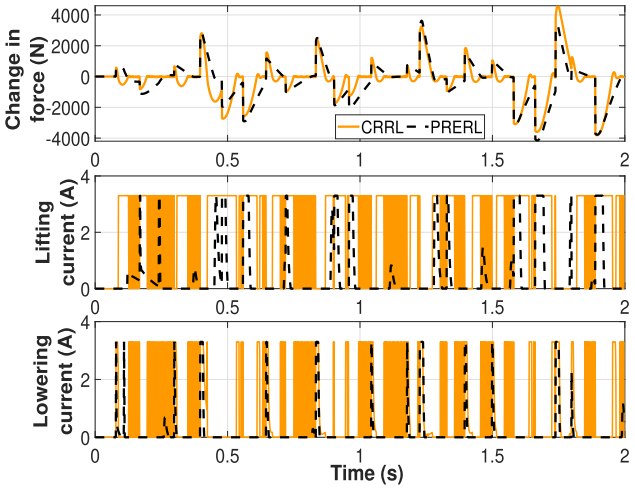

FIGURE 12. Comparison between CRRL and PRERL.

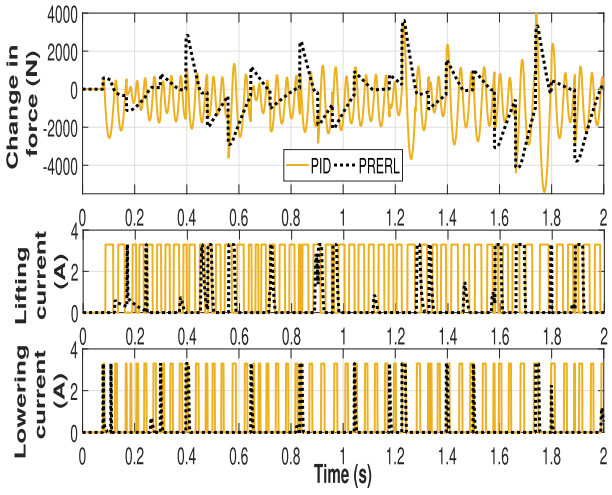

FIGURE 13. Comparison of the proposed SMC with PID controller.

lowering current, which is according to the trigger logic presented in Fig. 7. Also, the saturation imposed keeps the current input below 3.3 A. Variation of the position of the implement with the input is also shown. Average attenuation of 82.9% was obtained in the comparison between the controlled and uncontrolled systems. Attenuation was evaluated using the energy of the signal as,

$$A = \left[\frac{\sum_{n=1}^{N} \Delta f_{uc}{}^2 - \sum_{n=1}^{N} \Delta f_c{}^2}{\sum_{n=1}^{N} \Delta f_{uc}{}^2}\right] 100, \tag{26}$$

where A is the percentage attenuation, Δf_{uc} is the change in force without control and Δf_c is the change in force with

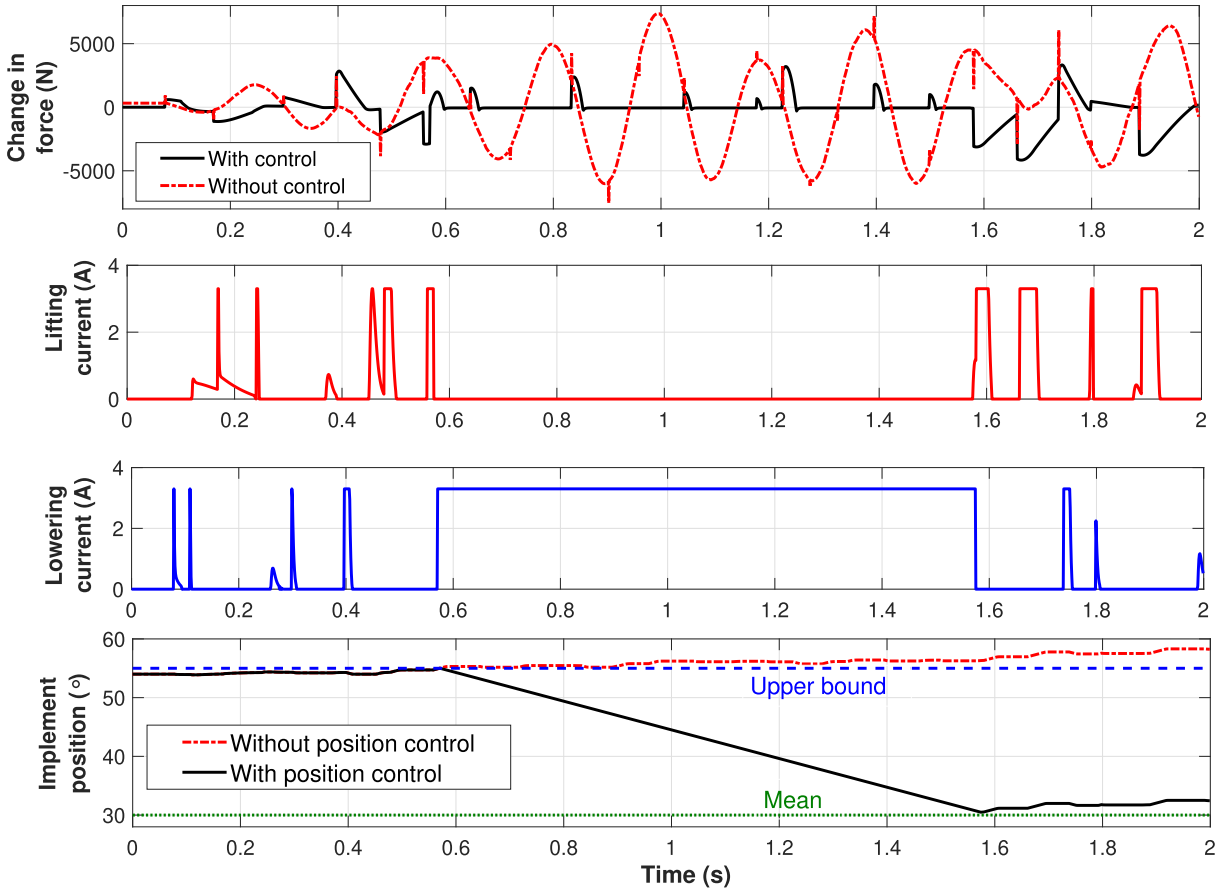

FIGURE 14. Position control demonstration.

control. The working of other aspects of the system is presented next.

A. SMC REACHING LAW COMPARISON

In order to identify the effectiveness of the PRERL based SMC, a comparison was made between CRRL and PRERL, which is shown in Fig. 12. Although the change in force response with both strategies is similar, CRRL produces chattering in the control input. As a consequence of chattering, there is overlap in the input to lifting and lowering valves, which is undesirable. PRERL provided up to 81% reduction in chattering in terms of magnitude as compared to CRRL.

B. PID CONTROL

A comparison with PID controller was made, since it was observed from the literature that PID control was extensively used in oscillation damping in hydraulic machinery. A PID controller was designed and tuned and tested with the same disturbance force as PRERL based SMC. The trigger logic, deadzone compensation, and current input saturation were also included. Comparison of system response and corresponding current input with both the control strategies are shown in Fig. 13. It can be observed that although

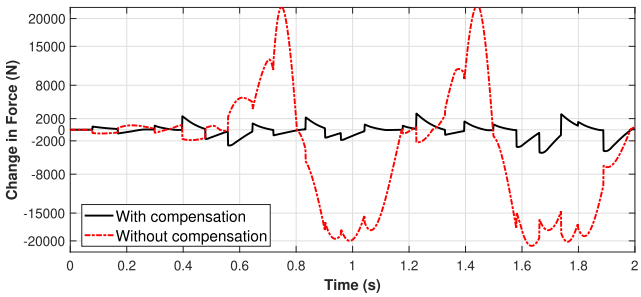

FIGURE 15. Deadzone effects.

the attenuation achieved in both strategies is comparable, the input current consumption is higher in case of PID. In SMC, the response is governed by $\dot{s}(t) = 0$, which is a first order differential equation. Therefore, the second order dynamics of the system is dominated by the first order dynamics of the sliding surface, which results in reduced oscillations in the system response. It can be observed that the system response with SMC has reduced oscillations as compared to PID.

C. POSITION CONTROL

In the previous tests, the hitch was considered to be kept at an initial position of 30°. But in practice, if the initial position

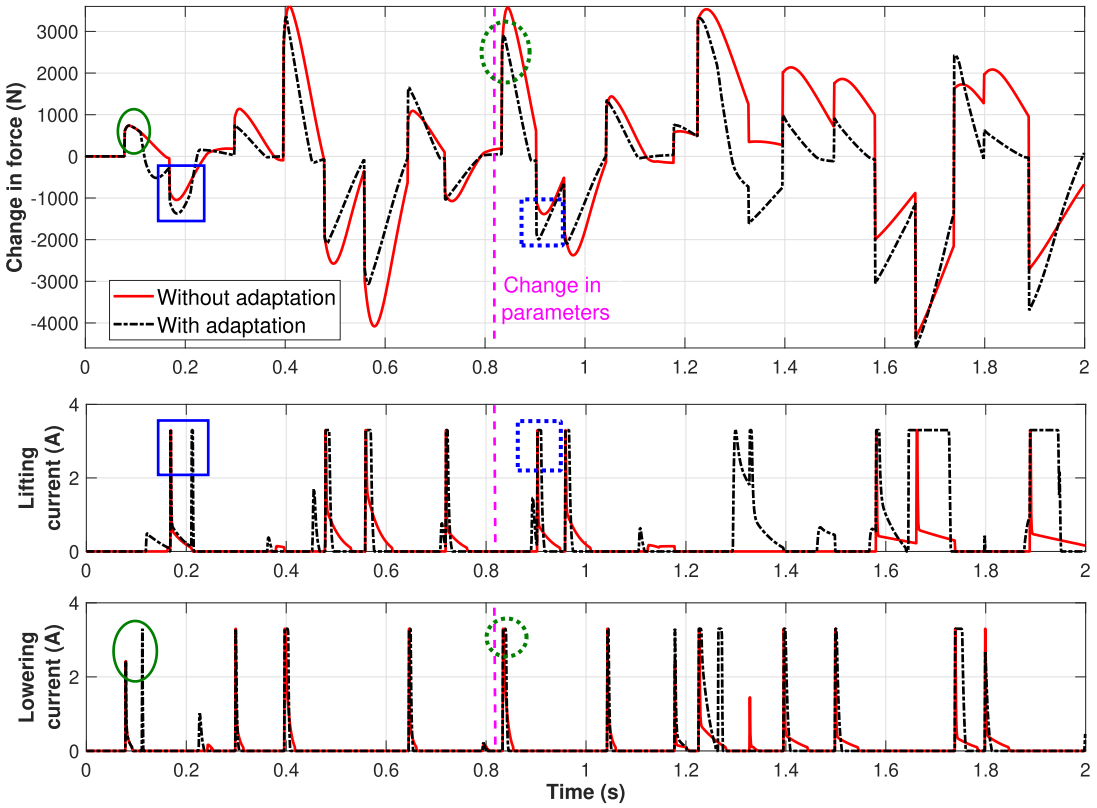

FIGURE 16. Comparison with and without parameter adaptation.

of the hitch is closer to the bounds, there is a possibility that the hitch might go out of bounds during control. This scenario was simulated to substantiate the working of position control. In Fig. 14, the initial position was kept closer to the upper bound of 55°. During operation, when the position went above 55°, the position controller was activated and it supplied current to the lowering valve till the implement was lowered to its mean position of 30°. Once the implement reached the mean position, force control was resumed. It can be observed from Fig. 14 that without position control, the implement moved past the upper bound.

D. DEADZONE EFFECTS

The adverse effects of not compensating for deadzone with closed loop control is shown in Fig.15. The system takes time to respond when deadzone is not compensated. During this time, there is a change of phase in the external disturbance force, but the system reacts to the disturbance measured earlier. Therefore, the force generated by the system adds to the disturbance rather than attenuating it, thus increasing the magnitude of force. It is seen that the performance without compensation is inferior compared to the case with deadzone compensation. Since the current input perceived by the system without compensation is lower, it makes the controller less effective. The system without deadzone compensation

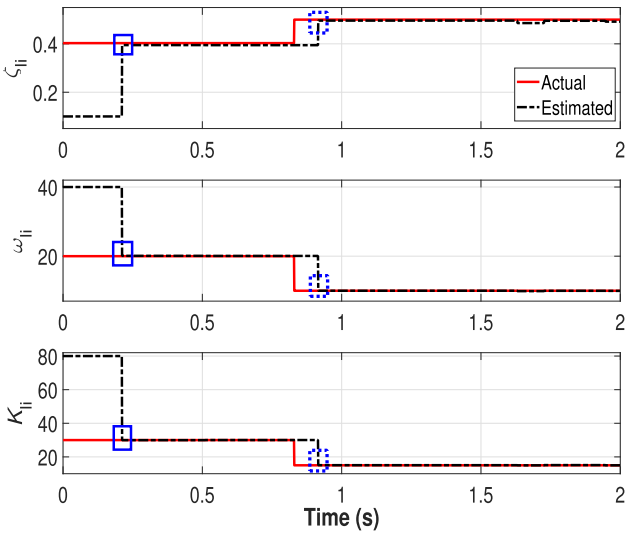

FIGURE 17. Online updated parameters (Lifting).

experienced 12% increase in energy of vibration signal, evaluated using Eq. 26, as compared to an uncontrolled system.

E. PARAMETER ADAPTATION

In order to evaluate the effectiveness of the parameter adaptation method, a test was carried out in which the plant parameters were varied. A comparison was made between

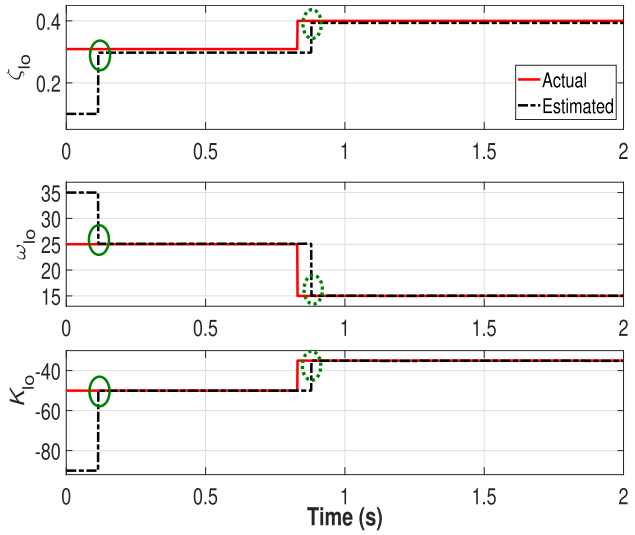

FIGURE 18. Online updated parameters (Lowering).

TABLE 5. Attenuation at different noise levels.

SNR (dB)	Attenuation (%)
No noise	82.91
30	81.33
25	79.89
20	62.64

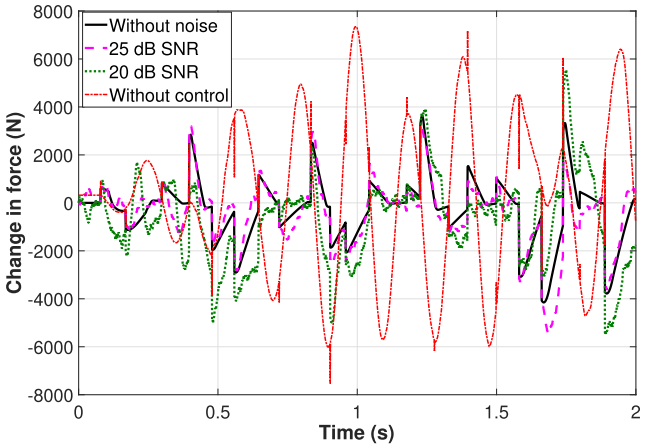

FIGURE 19. Noise sensitivity.

TABLE 6. Effect of parameter variation.

Parameter	Percentage variation	Range of values	Average attenuation (%)
ζ_{li}	-80 to 100	0.086 to 0.806	82.81
ω_{li}	-80 to 100	2.836 to 28.36	70.07
K_{li}	-80 to 100	3.82 to 38.2	81.37
ζ_{lo}	-80 to 100	0.0618 to 0.618	82.98
ω_{lo}	-80 to 100	4.038 to 40.38	78.88
K_{lo}	-80 to 100	-8.256 to -82.56	80.20

the response with and without parameter adaptation, which is shown in Fig. 16. It was found that attenuation was 11% better with parameter adaptation than without. During this comparison, the plant parameters were changed at 0.83 s.

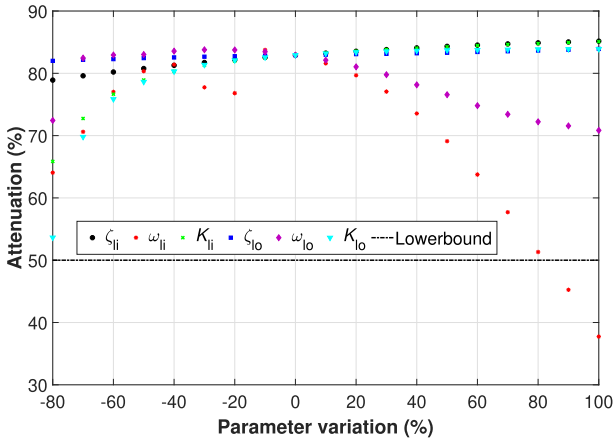

FIGURE 20. Robustness to parameter variation.

TABLE 7. Performance evaluation.

Quantity Evaluated	Method	Result		
State estimation error	MAPE	3.8% lifting and 7.5% lowering		
Parameter estimation error	MAPE	Parameter	Lifting	Lowering
		ζ	1.36%	2.82%
		ω	0.40%	0.37%
		K	0.22%	0.11%
Average attenuation	Energy of the signal	82.9%		
Chattering reduction	Energy of the signal	81%		
Deadzone effects	Difference in energy of the signal	12% increase without compensation		
Parameter adaptation	Difference in energy of the signal	11% lower with adaptation		
Noise sensitivity	Energy of the signal	SNR (dB)	Attenuation	
		No noise	82.91%	
		30	81.33%	
		25	79.89%	
		20	62.64%	
Robustness analysis	Energy of the signal	More than 50% attenuation with $\pm 80\%$ variation in parameters		

As per the rules in Fig. 10, the parameters were estimated only when the corresponding system (either lifting or lowering) was activated. Figures 17 and 18 indicate the points at which the estimates converged and the corresponding region is indicated in Fig. 16. It can be observed from these figures that the lowering system was activated first after the plant parameters changed (dotted circle), and hence the corresponding parameters were estimated. When the lifting system was subsequently actuated (dotted square), its parameters were estimated. It could be observed that the parameter estimation scheme performed well and the estimates converged to the actual values as soon as the corresponding system was activated in other cases as well (solid circle and solid square). In real time application, the measured force sensor signal and the input given to the valve are supplied to the

on-board parameter estimator. The estimator performs multiple iterations to obtain the values of the parameters. Since the actual values of the parameters are unknown, convergence criteria are predefined based on the system characteristics. Once the convergence criteria are met, the parameter values are updated in the controller. The convergence criteria were chosen such that the estimates converge as fast as possible with the estimation error being less than $\pm 1\%$.

F. NOISE SENSITIVITY ANALYSIS

A measurement noise was added to the change in force output to carry out the noise sensitivity analysis. In practice, a signal to noise ratio (SNR) of 20 dB is commonly considered as a weak signal [58] and SNR 25 dB and above is considered a good signal. Therefore, a noise value corresponding to SNR of 20 dB and 25 dB was added to the output and the response is shown in Fig. 19. It can be observed that at 25 dB, the response is close to response with no noise, and at 20 dB, the performance has deteriorated which is expected because of comparatively low signal quality. Table 5 gives the attenuation achieved with different noise levels.

G. ROBUSTNESS ANALYSIS

Robustness of the SMC with parameter estimation was studied by varying the system parameters for lifting and lowering one at a time. Table 6 shows the percentage and the range in which the parameters were varied. It also shows the average attenuation obtained while varying each parameter. The variation of attenuation with parameters is shown in Fig. 20. It was found that variation in ω has a higher effect on the performance. In the literature, the attenuation level reported is of the order of 40 % [10], [17], [18], [20]. Based on this, a lower bound for attenuation was considered to be 50 %. According to this, the controller was able to provide more than 50% attenuation with $\pm 80\%$ variation in parameters.

V. CONCLUSION

This research work focused on attenuating the disturbances forces on a farm tractor with an implement. Experimental data were used to obtain a second order transfer function model, which was then used to develop a robust controller for attenuating the disturbance forces. The constraints on position and current input were incorporated. The performance evaluation carried is summarized in Table 7 and key aspects of the study are listed below.

- SMC with an advanced reaching law, PRERL, was incorporated for disturbance attenuation, and it was found to reduce chattering by 81 % in comparison with CRRL.
- The controller resulted in average attenuation of 82.9 %, which is a significant improvement over existing techniques.
- The system was found to be robust to a parametric variation of $\pm 80\%$, and to perform satisfactorily in the presence of noise.
- The deadzone compensation technique successfully minimized the adverse effects of deadzone.
- The control input and the position of the implement were kept within the practical operating limits.
- The average estimation error for the Kalman filter state estimator and RLS parameter estimator used in the system was 5.6 % and 0.88 % respectively.
- The system can be incorporated on a tractor with an electro-hydraulic hitch to attenuate the disturbances.
- Robustness and adaptive capability enable the system to work with a wide range of loads and implements.
- The frame work can also be incorporated on off-road hydraulic machinery where oscillation damping is required.

REFERENCES

[1] "Ministry of agriculture and farmers welfare," Dept. Agricult., Cooperation Farmers Welfare, Government India, Krishi Bhawan, New Delhi, India, Annu. Rep. 2016-2017, 2017.
[2] U.S. Geological Survey. (2015). *Map of Croplands in the United States*. [Online]. Available: https://www.usgs.gov/media/images/map-croplands-united-states
[3] National Bureau of Statistics of China. (2015). *China Statistical Yearbook*. [Online]. Available: http://www.stats.gov.cn/tjsj/ndsj/2015/indexeh.htm
[4] S. K. Mandal and A. Maity, "Current trends of Indian tractor industry: A critical review," *Appl. Sci. Rep.*, vol. 3, no. 2, pp. 132–139, 2013.
[5] V. Baregal and D. K. Grover, "A quantitative analysis of demand for tractors in India," *Agricult. Update*, vol. 12, no. 3, pp. 764–769, Sep. 2017.
[6] K. Sim, H. Lee, J. W. Yoon, C. Choi, and S.-H. Hwang, "Effectiveness evaluation of hydro-pneumatic and semi-active cab suspension for the improvement of ride comfort of agricultural tractors," *J. Terramech.*, vol. 69, pp. 23–32, Feb. 2017.
[7] M. Bovenzi and A. Betta, "Low-back disorders in agricultural tractor drivers exposed to whole-body vibration and postural stress," *Appl. Ergonom.*, vol. 25, no. 4, pp. 231–241, 1994.
[8] P. Servadio, A. Marsili, and N. P. Belfiore, "Analysis of driving seat vibrations in high forward speed tractors," *Biosyst. Eng.*, vol. 97, no. 2, pp. 171–180, Jun. 2007.
[9] B. Stojić, N. Poznanović, and A. Poznić, "Research and modeling of the tractor tire enveloping behavior," *J. Vib. Control*, vol. 23, no. 2, pp. 290–304, Feb. 2017.
[10] D. Cristofori, A. Vacca, and K. Ariyur, "A novel pressure-feedback based adaptive control method to damp instabilities in hydraulic machines," *SAE Int. J. Commercial Vehicles*, vol. 5, no. 2, pp. 586–596, 2012.
[11] N. Mizoguchi, H. Asada, D. Kozuka, K. Ikei, and S. Hori, "Travel vibration suppressing device for working vehicle," U.S. Patent 7 621 124 B2, Nov. 24, 2009.
[12] R. Rahmfeld and M. Ivantysynova, "An overview about active oscillation damping of mobile machine structure," *Int. J. Fluid Power*, vol. 5, no. 2, pp. 5–24, Jan. 2004.
[13] A. Orbach and W. L. Schubert, "Active roadibility control for work vehicles," U.S. Patent 5 884 204, Mar. 16, 1999.
[14] K. B. Patel, H. C. Lin, W. Farag, and A. A. Khan, "EDC draft force based ride controller," U.S. Patent 6 196 327 B1, Mar. 6, 2001.
[15] S. Mizui, "Device and method for suppressing vibration of a working machine," U.S. Patent 5 832 730, Nov. 10, 1998.
[16] A. D. Berger and K. B. Patel, "Electronic ride control system for off-road vehicles," U.S. Patent 5 897 287, Apr. 27, 1999.
[17] J. Zhang and S. Chen, "Modelling and study of active vibration control for off-road vehicle," *Vehicle Syst. Dyn.*, vol. 52, no. 5, pp. 581–607, May 2014.
[18] A. Alexander, A. Vacca, and D. Cristofori, "Active vibration damping in hydraulic construction machinery," *Procedia Eng.*, vol. 176, pp. 514–528, Jan. 2017.
[19] T. O. Andersen, M. R. Hansen, and F. Conrad, "Robust control of oscillations in agricultural tractors," in *Proc. ASME Int. Mech. Eng. Congr. Expo.* New York, NY, USA: American Society of Mechanical Engineers, 2003, pp. 89–95.
[20] C. Williamson, S. Lee, and M. Ivantysynova, "Active vibration damping for an off-road vehicle with displacement controlled actuators," *Int. J. Fluid Power*, vol. 10, no. 3, pp. 5–16, Jan. 2009.